



ELSEVIER

Contents lists available at ScienceDirect

Journal of Solid State Chemistry

journal homepage: www.elsevier.com/locate/jssc

Luminescent lanthanide coordination polymers synthesized *via in-situ* hydrolysis of dimethyl-3,4-furandicarboxylate



Natalie E. Greig^a, Jeffrey D. Einkauf^a, Jessica M. Clark^a, Eric J. Corcoran^a, Joseph P. Karram^a, Charles A. Kent^a, Vadine E. Eugene^a, Benny C. Chan^b, Daniel T. de Lill^{a,*}

^a Department of Chemistry & Biochemistry, Florida Atlantic University, 777 Glades Road, Boca Raton, FL 33431, USA

^b Department of Chemistry, The College of New Jersey, 2000 Pennington Road, Ewing, NJ 08628, USA

ARTICLE INFO

Article history:

Received 7 October 2014

Received in revised form

13 January 2015

Accepted 17 January 2015

Available online 29 January 2015

Keywords:

Coordination polymers

Lanthanide luminescence

Quantum yield

Crystal structure

ABSTRACT

Dimethyl-3,4-furandicarboxylate undergoes hydrolysis under hydrothermal conditions with lanthanide (*Ln*) ions to form two-dimensional coordination polymers, $[Ln(C_6H_2O_5)(C_6H_3O_5)(H_2O)]_n$ (*Ln* = Sm, Eu, Gd, Tb, Dy, Ho, Er, Tm, Yb, Lu). The resulting materials exhibit luminescent properties with quantum yields and lifetimes for the Eu(III) and Tb(III) compounds of $1.1 \pm 0.3\%$ and 0.387 ± 0.0001 ms, and $3.3 \pm 0.8\%$ and 0.769 ± 0.006 ms, respectively. Energy values for the singlet and triplet states were determined for dimethyl-3,4-furandicarboxylate and 3,4-furandicarboxylic acid. Excited state dynamics and structural features are examined to explicate the reported quantum yields. A series of other FDC structures is briefly presented.

© 2015 Elsevier Inc. All rights reserved.

1. Introduction

Coordination polymers (CPs) are of great research interest due in part to the robust diversity of structural topologies [1–3]. These materials consist of metal centers bound together by organic linker moieties that come together to form structures of higher dimensionality. Of the metals used to synthesize these materials, lanthanides (*Ln*s) stand out for their potential applications in several fields, including magnetic materials and display technologies [4–6]. With an almost complete lack of crystal field effects, however, coordination of lanthanides is primarily electrostatic and nondirectional, making it difficult to predict the final structural topology when synthesizing new materials [7–9]. This is unlike transition metal containing structures, in which *d*-orbital mediated bonding grants predictable geometries and structures [10–13].

We are interested in studying the luminescence that arises in these compounds [14]. While direct excitation of *Ln* ions is inefficient, it is possible to attain highly luminescent materials through an indirect population of the *f*-excited state [15,16]. This sensitized emission is commonly referred to as the antenna effect, where a coordinated organic compound absorbs incident radiation and through a variety of steps that energy is transferred directly into the lanthanide's excited state. While this phenomenon has been studied for well over half

a century and many aspects of it understood, researchers still rely heavily on trial-and-error procedures in order to develop highly luminescent materials. It has been noted that the final photophysical behavior of lanthanide complexes is greatly dependent on the local geometry of the central *Ln* ion [17]. In particular, the precise geometric arrangement of the sensitizing organic species is critical, with variations in bond lengths of 0.01 Å showing measurable effects in the sensitization efficiency. CPs are ideal candidates in which to study the antenna effect in detail, yet there are few substantial quantitative reports of *Ln*-based luminescence on such compounds [8,14,18–24]. The primary advantage of studying these materials is that there is a direct correlation between structure and luminescence, whereas in complexes this correlation is an easily overstated assumption; it is convenient to presume that the solid-state structure is a reliable model of the complex in solution even though this may not necessarily be the case. Our research efforts focus on synthesizing CPs in order to better understand how to best utilize the antenna effect in producing more efficient luminescent materials with feasible applications in display technologies, telecommunications, and sensing. Our initial efforts toward this endeavor involved a structurally related pyridinedicarboxylate compound [14]. The pyridine-based compound showed unremarkable luminescence efficiency, prompting investigations into other heterocyclic-based compounds such as furan-based linkers to observe the effects such a linker would have. Herein, we report the hydrothermal synthesis [25], structure, and photophysical characterization of a 2D *Ln*-CP ($[Ln(C_6H_2O_5)(C_6H_3O_5)(H_2O)]_n$) made by *in-situ* ligand hydrolysis [26,27] (Scheme 1) of

* Corresponding author.

E-mail address: ddelill@fau.edu (D.T. de Lill).

dimethyl-3,4-furandicarboxylate (FDC, compound **1**). Compound **1** can be made across the *Ln* series, as confirmed by PXRD (*Ln*=Sm, Eu, Gd, Tb, Dy, Ho, Er, Tm, Yb, Lu). Syntheses using La, Ce, Pr, and Nd salts were unsuccessful, producing no solid compound at the end of the reaction.

2. Materials and methods

2.1. Crystallography

Single crystals were mounted on glass fibers for data collection. Reflections were collected at 100 K on a Bruker AXS SMART diffractometer equipped with an APEXII CCD detector using Mo K α radiation. Data was integrated using the Bruker program SAINT [28] and corrected for absorption using the SADABS [29] program. The structures of *Ln*-FDC were solved using the SIR92 [30] program and refined using SHELX-97 [31] within the WINGX [32] software suite. Crystallographic information for both coordination polymers is given in Table 1.

2.2. Synthesis

Coordination polymer ([Eu(C₆H₂O₅)(C₆H₃O₅)(H₂O)]_n) was synthesized from a solution of europium nitrate salt (Eu(NO₃)₃·6H₂O, 122.6 mg, 0.275 mmol) and dimethyl-3,4-furandicarboxylate (C₈H₈O₅, 50 mg, 0.275 mmol) in 3 mL of H₂O in a 23 mL Teflon lined autoclave. Aqueous potassium hydroxide (5 M KOH) was added to adjust the pH to 7–9. After 3 days (72 h) of hydrothermal conditions at 120 °C, the solution was decanted from the clear, colorless crystals, and washed twice with water and ethanol, after which they were allowed to air dry at room temperature. This compound was also successfully prepared using TbCl₃·6H₂O. Nitrate or chloride salts were used to synthesize the other *Ln* analogs. The resulting isostructural Tb- and Eu-CPs are orthorhombic and crystallize in the *Pbca* space group. Elemental analyses were conducted on both samples by Galbriath Laboratories, Inc., Knoxville, TN, USA. For the Eu compound: C (theoretical/actual), 30.08/30.06 and H, 1.47/1.50. For the Tb compound: C, 29.65/28.82 and H, 1.45/1.40.

2.3. Photophysical measurements

Quantum yields were determined from the following equation [33]:

$$\Phi_x = \frac{1 - R_x}{1 - R_{ST}} \times \frac{I_{ST}}{I_x} \times \Phi_{ST}$$

where *x* is the sample measured and ST is a standard with known Φ . The standard, pyrene, along with the sample and the matrix material,

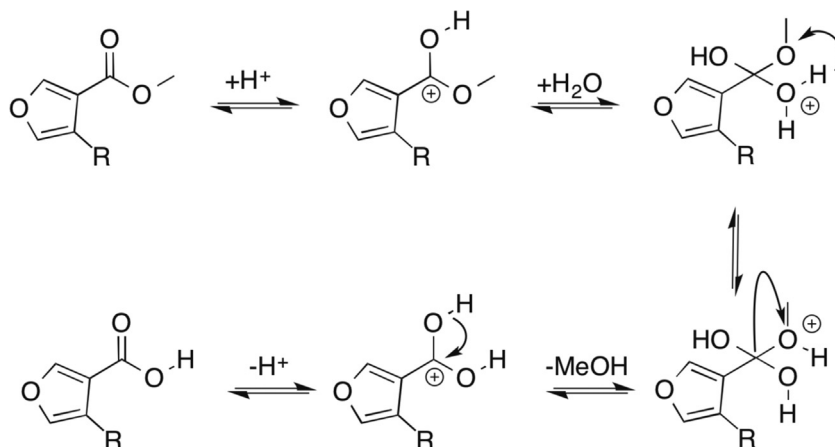
PMMA (poly (methyl methacrylate), avg. molecular weight ~15,000 by GPC) were all measured using a Perkin Elmer LS55 Fluorescence Spectrometer at room temperature (23 ± 2 °C). All samples were ground with PMMA to reduce the possibility of self-absorbance of emitted light and to avoid refractive index corrections to the quantum yields. Solid-state reflectance values were measured using a 60 mm integrating sphere on a Perkin Elmer Lambda 850 UV/Vis Spectrometer by scanning the emission monochromator through the specific excitation wavelength. The *I* values are found from the integrated emission profile of both pyrene and the sample. Using the known quantum yield of the standard, Φ_{ST} (61% at 313 nm excitation), the quantum yields of the sample were calculated. Integrations were performed using OriginPro 8.1 software. Lifetime measurements were collected using the BioLight Fluorescence Application software and analyzed in Origin Pro 8.1.

Singlet and triplet states of the organic moieties were measured using the fluorimeter to obtain approximate values of these energies of the sensitizer, where emission spectra were recorded with time delays of 0 to 0.05 ms from 315 to 700 nm at 272 nm excitation to distinguish between linker fluorescence and phosphorescence. Spectra were deconvoluted using OriginPro 8.1, where peak spacing was approximately equal to the furan ring skeleton

Table 1
Crystallographic information for Eu and Tb CPs.

Formula	[Eu(C ₆ H ₂ O ₅)(C ₆ H ₃ O ₅)(H ₂ O)] _n	[Tb(C ₆ H ₂ O ₅)(C ₆ H ₃ O ₅)(H ₂ O)] _n
Formula weight (g/mol)	479.15	486.11
Crystal class	Orthorhombic	Orthorhombic
Space group	<i>Pbca</i>	<i>Pbca</i>
<i>a</i> (Å)	15.122(2)	15.0789(15)
<i>b</i> (Å)	9.3656(14)	9.2997(9)
<i>c</i> (Å)	20.290(3)	20.287(2)
α (deg)	90	90
β (deg)	90	90
γ (deg)	90	90
<i>Z</i>	8	8
Cell volume (Å ³)	2873.7(8)	2844.8(5)
Density (mg m ⁻³)	1.933	2.270
μ (mm ⁻¹)	4.354	7.452
<i>R</i> _{int}	5.18%	6.01%
<i>R</i> ₁	2.37%	2.98%
w <i>R</i> ₂	6.08%	5.77%
GO _F	0.715	1.028
Total reflections	30,125	31,725

$$R_1 = \sum \frac{|F_o| - |F_c|}{|F_o|}; wR_2 = \left(\frac{\sum w(F_o^2 - F_c^2)^2}{\sum wF_c^2} \right)^{1/2}$$



Scheme 1. Typical mechanism of ester hydrolysis using the FDC linker as an example. The authors do not imply that this is the exact mechanism occurring within the synthesis of **1**, but is provided to give chemical justification of the hydrolysis.

vibrational modes ($1610\text{--}1475\text{ cm}^{-1}$). Singlet and triplet state values are reported as the 0–0 transitions from linker emission.

2.4. Further characterization

Thermogravimetric analysis was conducted on the Eu-analog of 1 using a Mettler-Toledo TGA/DSC 1 from 30 to 600 °C at 10 °C/min under a nitrogen gas flow. FTIR spectroscopy was likewise conducted on the Eu-analog of 1 to establish the vibrational modes present within the crystalline lattice. A ThermoScientific Nicolet iS5 FT-IR was used for this analysis.

3. Results and discussion

3.1. Structural description

The following structural description will focus specifically on that of the Eu-FDC CP. The other FDC CPs were found to have the same structure, as confirmed with single and/or powder X-ray diffraction. The title material is a two-dimensional compound constructed from EuO_8 polyhedra in a distorted square antiprism geometry that edge share to form a dimer. Surrounding each Eu, there are five monodentate oxygen atoms, which belong to carboxylate moieties (O1, O3, O4, O7, O8), two symmetry equivalent oxygen atoms (O2, also a carboxylate oxygen) bridging the Eu ions to form the dimer unit, and one bound water molecule (O9).

The Eu dimers form 2D sheets that expand along the [100] and [010] (Fig. 1) directions, propagated by the organic linker. These sheets (Fig. 2) stack along [001]. Fully protonated carboxylic acid groups are found dangling between the sheets, with carbon(C5)–oxygen bond distances of 1.223 Å (C=O) and 1.312 Å (C–OH) for O10 and O11, respectively. H-bonding and $\pi\text{--}\pi$ interactions facilitate the stacking of the sheets.

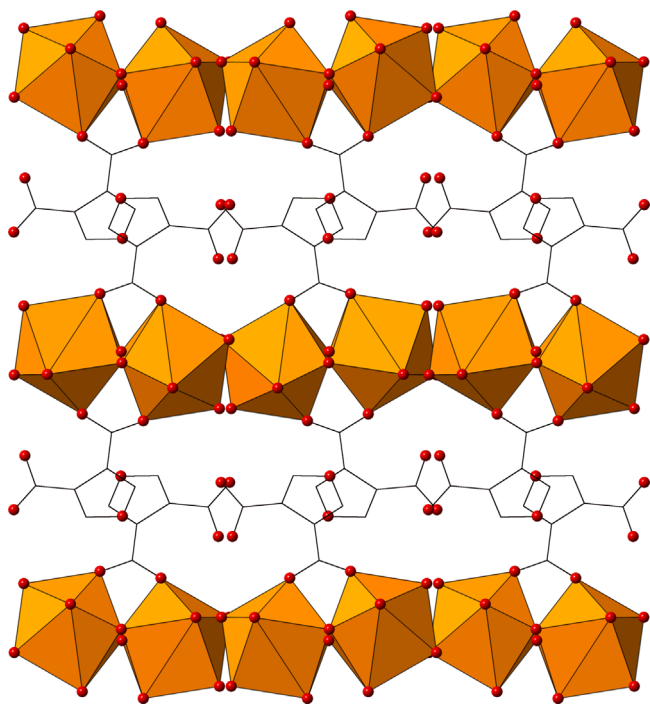


Fig. 1. View of the title compound down [010], showing the stacking of the layers. Note the uncoordinated FDC in between the layers. Orange polyhedra represent Eu (III), black lines are carbon, and red spheres are oxygen. Hydrogens have been omitted for clarity. (For interpretation of the references to color in this figure legend, the reader is referred to the web version of this article.)

The structure contains two crystallographically unique FDC linkers. The first FDC coordinates to both lanthanides of the dimer and provides one oxygen to each lanthanide center in a monodentate fashion from only one of its carboxylate moieties, O3 and O4. This coordination is mirrored by a symmetrically equivalent FDC ligand at an angle of 134.04°. The remaining carboxylate moiety of this FDC remains uncoordinated and is protonated, and lies in between and nearly orthogonal to the sheets. FTIR spectroscopy shows both protonated and deprotonated FDC (see SI). The second FDC linker acts to propagate the sheets and is entirely coordinated to the lanthanides through all carboxylate oxygen atoms. Bridging the two lanthanide ions of the dimer is a bidentate oxygen atom, O2, of a carboxylate group. The remaining oxygen of this carboxylate group, O1, is coordinated to one Eu, while the other dimer receives coordination through O1' with a symmetrically equivalent ligand on the opposite side of the dimer, along with an O2' bridge repeated on the other side. The other carboxylate of this linker operates to connect two neighboring dimer groups, with O8 bonding to a Eu of one dimer, and O7 coordinating to a Eu of the next nearest dimer. The last coordinated moiety, the bound water, O9, is in roughly the same plane as O2 and O3. Table 2 notes selected bond lengths for the title compounds. Fig. 3 shows a ball-and-stick representation of the dimer unit, and Fig. 4 shows the thermal ellipsoid plots for the crystallographically unique atoms.

Table 3 shows the hydrogen bonding in the Eu-CP. First, there is a hydrogen bond between the bound water ligand O(9) and O(1) of the fully deprotonated FDC that forms the dimer. The second interaction in the table is between O(10), which is a carboxylic acid moiety of one sheet dangling in the channel, and O(9), which is a bound water of a dimer on a neighboring sheet. This interaction aids in stacking the sheets. The next interactions involve weaker C–H-Acceptor hydrogen bonds. There is a weak intersheet interaction between C(8)–H(8) of the dangling furan moiety of one sheet to a coordinated oxygen of a dimer in a neighboring sheet, O(1). There is another weak H-bond between C(9) and O(10), occurring in the channels and is between two furan moieties of different sheets, further aiding in the stacking of the sheets. Lastly, there is a weak intrasheet hydrogen bond between C(11)–H(11) and the bound water molecule, O(9).

There is a $\pi\text{--}\pi$ interaction between two neighboring centroid Cg(2)–Cg(2) (calculated using PLATON [34] where Cg=ring center of gravity; values provide center to center distances) rings in which O6, C11, C10, C13, and C12 make up Cg(2). This interaction occurs at a distance of 3.560 Å, and is between two neighboring dimers within the sheet. A weak interaction between centroids Cg(1) and Cg(2), where Cg(1) is formed from the ring made up from atoms O5, C8, C4, C3, and C9. This intersheet interaction occurs at a distance of 4.014 Å and aids in the stacking of the sheets.

This structure is remarkably similar to a CP constructed by 2, 3-pyridinedicarboxylate (pydc) anions [14] instead of FDC ions. Both compounds are 2-D CPs constructed from Ln dimers with one fully deprotonated linker, one partially deprotonated linker, and one aqua ligand, just as with the title compound. The layers stack through similar hydrogen bonding interactions as well. The pydc compound displayed an interesting thermal decomposition, which seems to be mirrored within compound 1 as well (see SI for thermogram). Beginning at 100 °C, compound 1 (Eu) loses 10.1% of its mass, which can be attributed to the loss of the bound water ligand and a CO molecule (calculated loss of 9.6%). The CO is lost from the partially protonated linker. This linker continues to degrade over two nearly indistinguishable mass losses of 9.4% and 17.6% beginning at around 330 °C, corresponding to loss of a CO₂ moiety followed by the rest of the linker (calculated losses: CO₂=9.2%; C₄H₃O₂=17.3%). The compound continues to degrade immediately after these two mass losses to remove the rest of the organic species (experimental=27.9%; theoretical=27.1%). Overall, a mass loss of 65.0% was observed. This

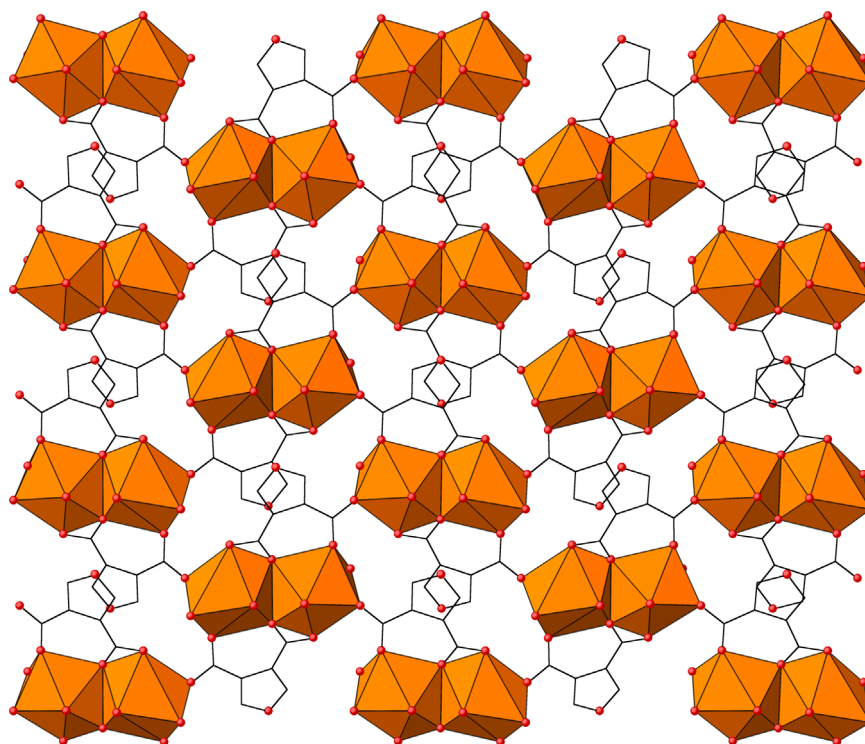


Fig. 2. The structure of an individual layer in the title compound. See Fig. 1 for color scheme. (For interpretation of the references to color in this figure legend, the reader is referred to the web version of this article.)

Table 2
Selected bond lengths for Eu and Tb CPs.

Eu-FDC Eu1–Ox		Tb-FDC Tb1–Ox	
X	Å	X	Å
8	2.276(2)	8	2.249(3)
7	2.292(2)	7	2.261(3)
2	2.369(2)	2	2.349(3)
4	2.387(2)	4	2.356(3)
9	2.415(2)	9	2.391(3)
3	2.431(2)	3	2.405(3)
1	2.500(2)	1	2.482(3)
2 ⁱ	2.521(2)	2 ⁱ	2.486(3)
C5–O10	1.223(4)	C5–O10	1.225(6)
C5–O11	1.312(5)	C5–O11	1.324(6)

Superscript *i*=symmetry operator $-x, -y, -z$.

corresponds to the expected end degradation product of Eu_2O_3 (theoretical mass loss total of 63.3%). This results suggests that lanthanide CPs of similar structure, regardless of composition, may follow similar thermal degradation pathways.

3.2. Photophysical studies

Excitation and emission spectra were collected for both prepared europium and terbium coordination polymers, and are seen in Figs. 5 and 6. The optimal excitation wavelength for both CPs is 272 nm, attributed to FDC excitation, with both showing characteristic Ln (III) emission profiles. The Eu compound shows the $^5\text{D}_0 \rightarrow ^7\text{F}_j$ transitions at 592, 615, 649, and 695 nm for $J=1, 2, 3,$ and 4. The Tb compounds shows the $^5\text{D}_4 \rightarrow ^7\text{F}_j$ transitions at 491, 546, 586, and 623 nm for $J=6, 5, 4,$ and 3. Solid-state quantum yields were determined against pyrene ($\Phi=61\%$ at $\lambda=313$ nm) in PMMA [21,33]. Quantum yields and lifetimes of both compounds were measured

several times to assure consistency. The determined quantum yields of the Eu- and Tb-CP were $1.1 \pm 0.3\%$ and $3.3 \pm 0.8\%$ with lifetimes of 0.387 ± 0.0001 ms and 0.769 ± 0.006 ms, respectively (Table 4).

Direct excitation of lanthanides is parity and often spin forbidden, leading to low molar absorptivities [35]. As such, indirect excitation pathways, such as the antenna effect, are used to facilitate more efficient excitation of these ions. Here, an organic moiety is used to absorb incident radiation and transfer it directly to the *f*-excited state of the Ln [15,16,36–39]. Values of the singlet and triplet state were estimated from the starting methyl ester using time resolved luminescence at room temperature in order to evaluate efficiency of energy transfer in the system [40]. The singlet and triplet state lie at approximately $29,610 \pm 170$ cm^{-1} and $21,900 \pm 150$ cm^{-1} . The singlet and triplet state energy values of the hydrolyzed linker were calculated using the Gaussian [41] program (B3LYP level of theory using the 6–31G basis set). The calculated singlet and triplet state of the carboxylic acid is $31,619$ cm^{-1} and $23,186$ cm^{-1} . To confirm these values, the methyl ester was hydrolyzed using dilute NaOH under reflux conditions, and protonated using dilute HCl. The final carboxylic acid was used to experimentally determine the singlet and triplet state values. It was difficult to resolve the difference between the ligand fluorescence and phosphorescence, but the singlet state was determined to lie at approximately $31,890$ cm^{-1} , while the triplet state appears to lie between $23,980$ and $25,350$ cm^{-1} . The singlet state matches quite well with the calculated value, and the lower range of the estimated triplet state also matches the calculated value well. The median value of this range, $24,665$ cm^{-1} will be used for the linker's triplet state in the following discussion. These values are summarized in Table 5.

For intersystem crossing (ISC) from the singlet to triplet state to effectively occur, the difference in energies should be greater than $5,000$ cm^{-1} , as is the case here ($\Delta E_{1S-3T} = 7910$ cm^{-1}) [33]. Therefore, the ISC in this system is efficient. For energy transfer (ET) from the triplet state to the *f*-excited state of the lanthanide to be efficient, the difference in energy should be in a range of 2500 – 3500 cm^{-1} for Eu(III) ($^5\text{D}_0 \sim 17,250$ cm^{-1}) and 2500 – 4000 cm^{-1} for Tb(III)

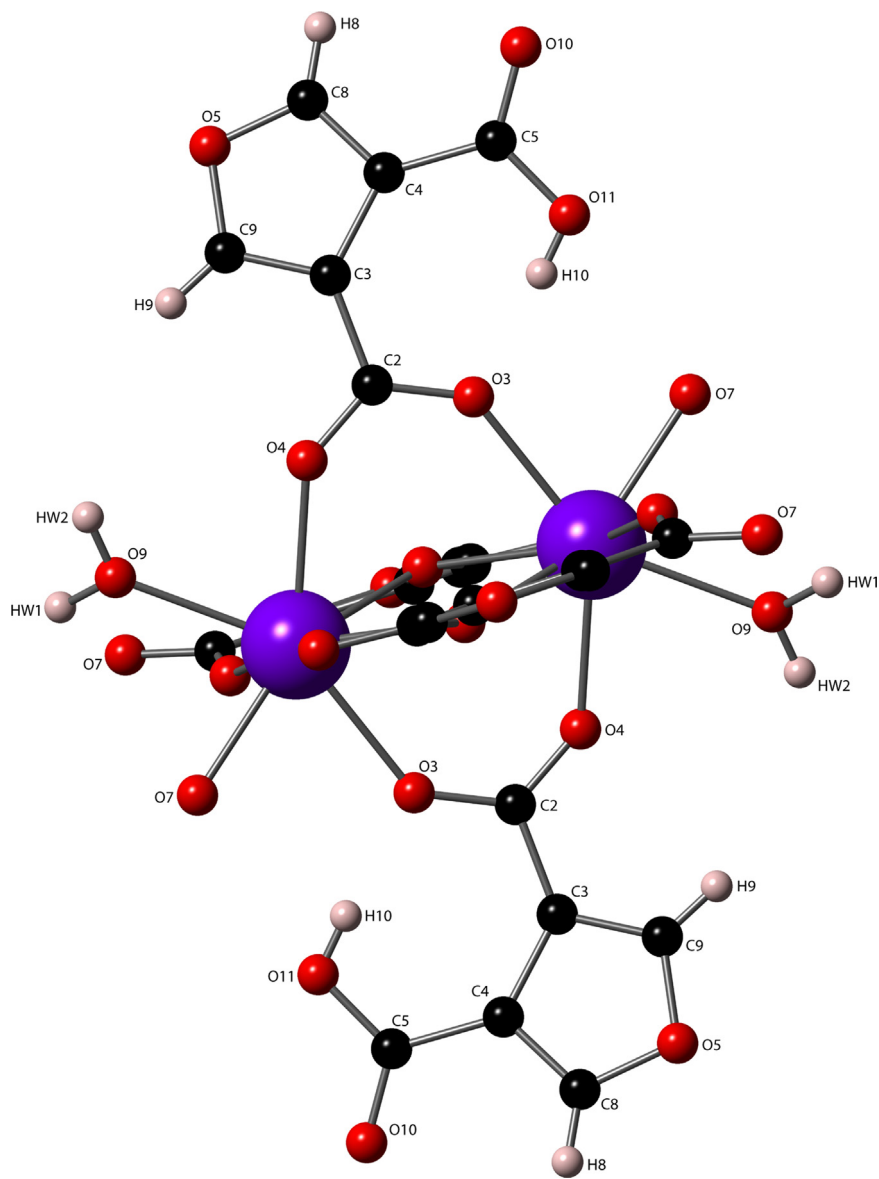


Fig. 3. Ball-and-stick representation of the Ln dimer unit, including hydrogen atoms (white). Carbon is black, oxygen is red, and the purple is the Ln center. (For interpretation of the references to color in this figure legend, the reader is referred to the web version of this article.)

(5D_4 20,430 cm^{-1}) [38]. From analysis of these values, it appears that in the case of Eu, ET is inefficient due to the energy difference between the two states being too great. On the other hand, the energy difference for that of the Tb system is between 3550 and 4920 cm^{-1} , with the median value of 4235 cm^{-1} . While the lower value is within the ideal range for energy transfer to the 5D_4 manifold of Tb, the median and upper values are above that range. Just the same, this rule is not absolute, and Latva [38] observed quantum yields between 20% and 60% for compounds whose triplet states exceeded 25,000 cm^{-1} . While it appears feasible that the FDC triplet state is at or above the upper range of energy to efficiently transfer energy to Tb, the extremely low quantum yields for this compound, particularly for Tb are likely due to additional reasons.

Some loss in efficiency may be attributed to the structure of the coordination polymer itself. Upon investigation of thermal ellipsoid plots (Fig. 4), uncoordinated carboxylic acids dangling in the channels were observed to undergo significant vibrations in the structure (even at 100 K), which can lead to phonon-assisted deactivation of the f -excited state. Hence, this deactivation mechanism is even more significant at room temperature (at which

luminescence experiments were conducted). Furthermore, the bound water already present in the material possesses vibrational modes that are well known to deactivate the excited state of the compound [42]. In solutions of Ln complexes, it is known that 3–4 O–H oscillators in proximity to the Ln ion can effectively quench Ln emission in trivalent Eu and Tb. Between the two oscillators directly bound to the Ln, and the O–H oscillator from the uncoordinated carboxylic acid, there is sufficient high-energy oscillators present to deactivate the Ln's excited state. FTIR spectroscopy further confirms the presence of these high-energy oscillators (See SI). Around 3450 cm^{-1} , hydrogen bound O–H stretches are observed, attributed to the bound aqua ligand. A shoulder around 3250 cm^{-1} is likely the carboxylic acid alcohol stretch. Arene C–H stretches from the FDC furan ring are seen at ~ 3100 cm^{-1} . Added together, these oscillators are sufficient to bridge the gap between the f -excited states of Eu and Tb and their respective ground states (total $\sim 16,350$ cm^{-1} for 2 water O–H oscillators, 1 alcohol oscillator, and two C–H oscillators). Coupled with poorly matched singlet and triplet state values of the sensitizer, these factors all contribute to the poor quantum yields of these compounds.

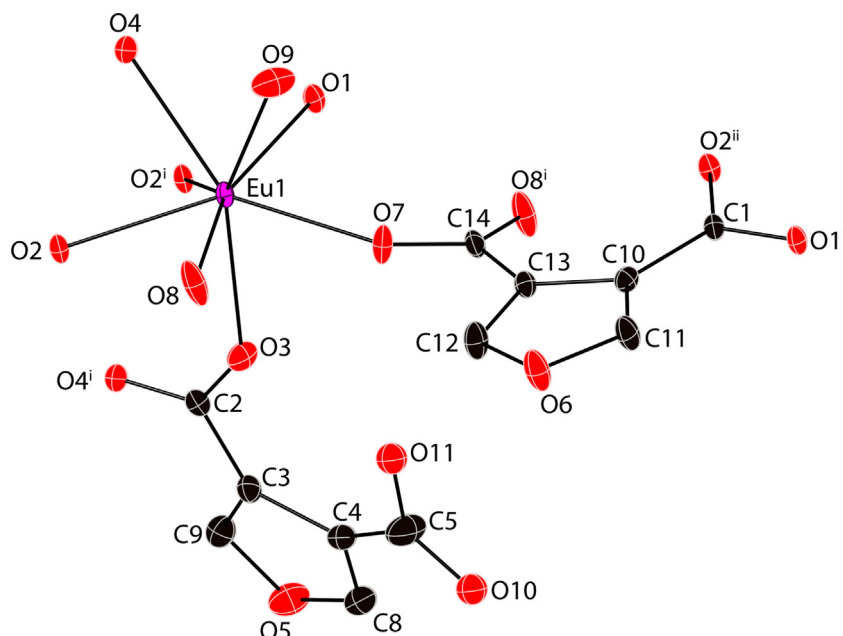


Fig. 4. Thermal ellipsoid plots (50% level) of all crystallographically unique atoms in Eu-FDC CP (symmetry equivalent atoms are denoted by superscripts: $i=2-x, -y, -z$; $ii=1.5-x, 1.5+y, z$). Note the larger thermal parameters for O10 and O11. Even at 100 K, there is significant thermal motion in these atoms that contribute to additional vibrational modes in the structure (especially at room temperature). Hydrogen atoms have been omitted.

Table 3
Hydrogen bonding geometric parameters (Å, deg).

Interaction	D⋯⋯A	D–H	H⋯⋯A	Angle
O(9)–Hw(1)⋯⋯O(1)	2.785(3)	0.96(5)	1.82(5)	178(4)
O(9)–Hw(2)⋯⋯O(10)	2.748(4)	0.88(4)	1.88(4)	173(4)
O(11)–H(10)⋯⋯O(3)	2.596(4)	0.82	1.78	176
C(8)–H(8)⋯⋯O(1)	3.241(4)	0.93	2.56	131
C(9)–H(9)⋯⋯O(10)	3.158(4)	0.93	2.26	162
C(11)–H(11)⋯⋯O(9)	3.442(4)	0.93	2.57	157

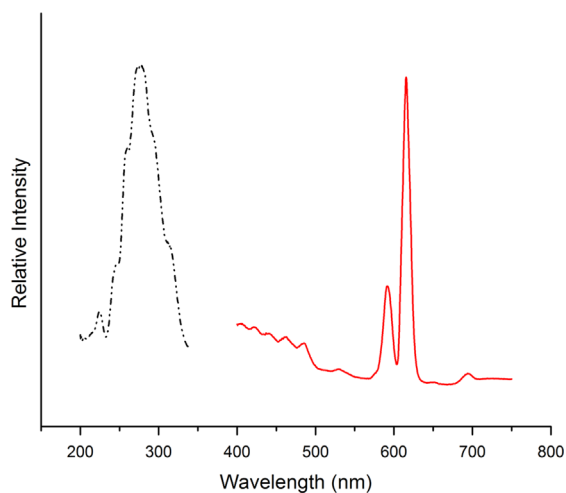


Fig. 5. Excitation (black) and emission (red) spectra of the title compound ($Ln=Eu$). (For interpretation of the references to color in this figure legend, the reader is referred to the web version of this article.)

3.3. Molecular modeling

The frontier orbitals of FDC-acid were modeled as well, as seen in Fig. 7. The HOMO is localized primarily on the furan ring demonstrating the π -bonding of the system. There is also some character from the carbonyl oxygen mixed with the HOMO. Since

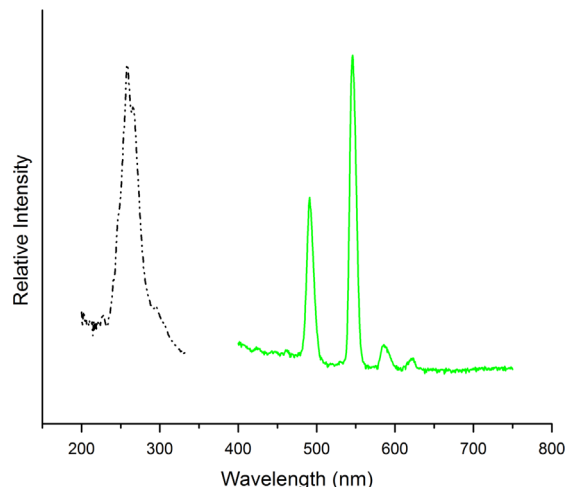


Fig. 6. Excitation (black) and emission (green) spectra of the title compound ($Ln=Tb$). (For interpretation of the references to color in this figure legend, the reader is referred to the web version of this article.)

Table 4
Quantum yields and lifetimes of the Eu and Tb analogs of the title compound.

	ϕ (%)	τ (ms)
Eu	1.1 ± 0.3	0.387 ± 0.0001
Tb	3.3 ± 0.8	0.769 ± 0.006

the LUMO is non-bonding in nature with localized electron densities from the oxygen lone pairs, the LUMO+1 was also modeled and clearly shows the π -antibonding orbitals of the FDC compound.

3.4. Other FDC compounds

The hydrolysis reaction that occurs *in-situ* creates byproducts that can be incorporated into the final structures through slight changes to the synthetic parameters. For compounds **2** and **3** (see SI), the

Table 5

Summary of the calculated and experimentally determined values for the first excited singlet and triplet states of the methylester-FDC and the carboxylic acid-FDC.

	$^1S_{\text{calculated}}$ (cm^{-1})	$^1S_{\text{experimental}}$ (cm^{-1})	$^3T_{\text{calculated}}$ (cm^{-1})	$^3T_{\text{experimental}}$ (cm^{-1})
FDC- ester	29,456	29,610	21,824	21,900
FDC- acid	31,619	31,890	23,186	23,980–25,350 ^a

^a Resolution between linker fluorescence and phosphorescence was difficult, but the triplet state is believed to be within this range.

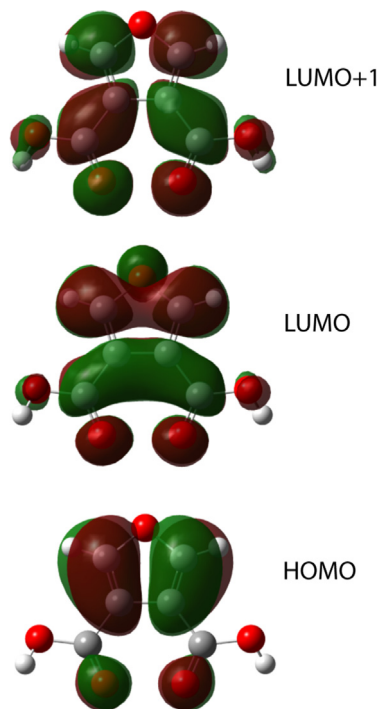


Fig. 7. Contour plots of the frontier orbitals of 3,4-furandicarboxylic acid, showing the HOMO (bonding), LUMO (nonbonding), and LUMO+1 (antibonding) molecular orbitals.

amount of water used was reduced to study the effects that the amount of water had on these reactions. Both compounds are two-dimensional materials that incorporated formate (**2**) and oxalate (**3**) ions into their structures. For compound **4**, NaCl was added to the same reaction as **1** in an attempt to introduce Na ions in between the layers of **1** though coordination to the carboxylic acids. Instead, a two-dimensional compound formed that integrated formate ions into the structure. Attempts to reproduce these compounds provided inconsistent results, and as such are reported merely to indicate that the hydrolysis byproducts can indeed become incorporated into such reactions. Synthetic and crystallographic details are provided in the SI.

4. Conclusion

In summary, two-dimensional Ln coordination polymers were prepared hydrothermally with 3,4-furandicarboxylate as a linker following *in-situ* ligand hydrolysis. Though it was determined that the structures exhibit lanthanide luminescence through organic excitation, the quantum yields of the materials were low, with values of $1.1 \pm 0.3\%$ and $3.3 \pm 0.8\%$ for the Eu- and Tb-CPs, respectively.

These quantum yields indicate that the furan moiety is not a highly efficient sensitizer of Ln(III) emission due to ill-suited triplet state values and the presence of high-energy oscillators in proximity to the Ln ion causing non-radiative decay. A series of oxalate or formate containing FDC compounds were briefly presented as well.

Acknowledgments

The authors would like to thank Florida Atlantic University for funding this project along with the NSF MRI Grant (No. 0922931). The authors would also like to thank Andrew Kerr and Dr. Christopher L. Cahill at The George Washington University for PXRD data, and Dr. Sharon Rivera for assistance with Gaussian. Many of the undergraduate students working on this project were funded through grants from FAU's Office of Undergraduate Research and Inquiry.

Appendix A. Supplementary information

Supplementary data associated with this article can be found in the online version at <http://dx.doi.org/10.1016/j.jssc.2015.01.014>.

TGA and IR of compound **1**; synthetic details and figures for compounds **2–4**; CIFs. This information is available free of charge via the Internet at <http://pubs.acs.org>. CCDC 896763 (Eu) and 896764 (Tb) also contain the supplementary crystallographic data (CIFs) for this paper. These data can be obtained free of charge from The Cambridge Crystallographic Data Centre via www.ccdc.cam.ac.uk/data_request/cif.

References

- [1] N.R. Champness, Dalton Trans. (7) (2006) 877.
- [2] C. Janiak, Dalton Trans. (14) (2003) 2781.
- [3] S.L. James, Chem. Soc. Rev. 32 (2003) 276.
- [4] C.J. Kepert, Chem. Commun. (7) (2006) 695.
- [5] S. Kitagawa, S.-I. Noro, T. Nakamura, Chem. Commun. (7) (2006) 701.
- [6] U. Mueller, M. Schubert, F. Teich, H. Puetter, K. Schierle-Arndt, J. Pastre, J. Mater. Chem. 16 (2006) 626.
- [7] D.T. de Lill, C.L. Cahill, Prog. Inorg. Chem. 55 (2007) 143.
- [8] C. Marchal, Y. Filinchuk, D. Imbert, J.-C.G. Bünzli, M. Mazzanti, Inorg. Chem. 46 (2007) 6242.
- [9] Z. Min, M.A. Singh-Wilmot, C.L. Cahill, M. Andrews, R. Taylor, Eur. J. Inorg. Chem. 28 (2012) 4419–4426.
- [10] M. O'Keefe, O.M. Yaghi, Chem. Rev. 112 (2012) 675.
- [11] N.L. Rosi, M. Eddaoudi, J. Kim, M. O'Keefe, O.M. Yaghi, Cryst. Eng. Commun. 4 (2002) 401.
- [12] M.J. Rosseinsky, Microporous Mesoporous Mater. 73 (2004) 15.
- [13] M. Eddaoudi, D.B. Moler, H. Li, B. Chen, T.M. Reineke, M. O'Keefe, O.M. Yaghi, Acc. Chem. Res. 34 (2001) 319.
- [14] A.L. Ramirez, K.E. Knope, T.T. Kelley, N.E. Greig, J.D. Einkauf, D.T. de Lill, Inorg. Chim. Acta 392 (2012) 46.
- [15] J.-C.G. Bünzli, Acc. Chem. Res. 39 (2006) 53.
- [16] J.-C.G. Bünzli, C. Piguet, Chem. Soc. Rev. 34 (2005) 1048.
- [17] L.N. Puntus, K.A. Lyssenko, M.Y. Antipin, J.-C.G. Bünzli, Inorg. Chem. 47 (2008) 11095.
- [18] X. Hu, W. Dou, C. Xu, X. Tang, J. Zheng, W. Liu, Dalton Trans. 40 (2011) 3412.
- [19] M.V. Lucky, S. Sivakumar, M.L.P. Reddy, A.K. Paul, S. Natarajan, Cryst. Growth Des. 11 (2011) 857.
- [20] A. de Bettencourt-Dias, Inorg. Chem. 44 (2005) 2734.
- [21] D.T. de Lill, A. de Bettencourt Dias, C.L. Cahill, Inorg. Chem. 46 (2007) 3960.
- [22] Y. Hasegawa, R. Hieda, K. Miyata, T. Nakagawa, T. Kawai, Eur. J. Inorg. Chem. 2011 (2011) 4978.
- [23] M.-X. Wang, L.-S. Long, R.-B. Huang, L.-S. Zheng, Chem. Commun. 47 (2011) 9834.
- [24] L. Ma, O.R. Evans, B.M. Foxman, W. Lin, Inorg. Chem. 38 (1999) 5837.
- [25] C.S. Cundy, P.A. Cox, Chem. Rev. 103 (2003) 668.
- [26] M.H. Alkordi, Y. Liu, R.W. Larsen, J.F. Eubank, M. Eddaoudi, J. Am. Chem. Soc. 130 (2008) 12639.
- [27] Y.-Q. Sun, J. Zhang, G.-Y. Yang, Chem. Commun. (2006) 1947.
- [28] SAINT; 5.053, Bruker Analytical X-Ray Systems, Inc., Madison, Wisconsin, 1998.
- [29] G.M. Sheldrick, SADABS 2.03, University of Gottingen, Germany, 2002.
- [30] A. Altomare, G. Casciarano, C. Giacovazzo, A.J. Guagliardi, Appl. Crystallogr. 26 (1993) 343.

- [31] G.M. Sheldrick, SHELX97, Institut für Anorganische Chemie der Universität, Tammanstrasse 4, D-3400 Göttingen, Germany, 1998.
- [32] L.J. Farrugia, *J. Appl. Crystallogr.* 32 (1999) 837.
- [33] A. Brill, A.W. de Jager-Veenis, *J. Res. Natl. Bur. Stand. (US) Sec. A 80A* (1976) 401.
- [34] A.L. Speck, *Acta Crystallogr. Sect. A* 46 (1990) C34.
- [35] H.C. Aspinall, *Chemistry of the f-Block Elements*, CRC, 2001.
- [36] D. Parker, *Chem. Soc. Rev.* 33 (2004) 156.
- [37] A. de Bettencourt-Dias, *Dalton Trans.* (22) (2007) 2229.
- [38] M. Latvaa, H. Takalob, V.-M. Mikkala, C. Matachescu, J.C. Rodriguez-Ubis, J. Kankarea, *J. Lumin.* 75 (1997) 149.
- [39] M.D. Allendorf, C.A. Bauer, R.K. Bhakta, R.J.T. Houk, *Chem. Soc. Rev.* 38 (2009) 1330.
- [40] G.A. Crosby, R.E. Whan, R.M. Alire, *J. Chem. Phys.* 34 (1961) 743.
- [41] GaussView, Version 5, Roy Dennington, Todd Keith, and John Millam.
- [42] G.R. Choppin, D.R. Peterman, *Coord. Chem. Rev.* 174 (1998) 283.